Hindawi
Shock and Vibration
Volume 2018, Article ID 4979405, 10 pages
https://doi.org/10.1155/2018/4979405

Research Article

Prediction and Analysis of Polished Rod Dynamometer Card in Sucker Rod Pumping System with Wear

Dongyu Wang and Hongzhao Liu

School of Mechanical and Precision Instrument Engineering, Xi'an University of Technology, Xi'an 710048, China

Correspondence should be addressed to Hongzhao Liu; liu-hongzhao@163.com

Received 4 July 2018; Revised 21 September 2018; Accepted 2 October 2018; Published 1 November 2018

Academic Editor: José J. Rangel-Magdaleno

In the oil production process, the wear of friction pairs in sucker rod pumping installations will increase over time, which leads to the failure of the sucker rod pumping system. In order to study the effect of wear on the sucker rod pumping system, a wear model between the plunger and pump barrel was established. By analyzing the wear law, the wear volume and wear time of the pump barrel were calculated under abrasive wear. The forces of the sucker rod microunit were analyzed, and the wave equation of the sucker rod was established. Based on the given boundary and initial conditions, a mixed difference method was used to solve the equation. Taking the no. L2111 well of an oilfield as an example, the change curves of the wear volume and wear time with abrasive particle diameter were plotted, and the polished rod dynamometer card considering wear was predicted. The results showed that the increased clearance caused by wear will reduce the polished rod load on upstroke of the sucker rod pumping system, which could provide a theoretical basis for the next fault diagnosis.

1. Introduction

The petroleum industry plays an important role in the continuous development of the national economy. The state has attached great importance to the petroleum industry and issued the 13th five-year plan for oil development in 2016 [1]. The process of petroleum exploration, mining, processing, and exploitation are the key activities of the petroleum industry. At present, the use rod pumping equipment is the main means of oil recovery, among which the pumping unit is one of the main working parts. Among the parameters of the pumping unit, the polished rod load is the most common and most important. The polished rod dynamometer card is an image describing the change in the polished rod load with polished rod displacement. It not only reflects the downhole working conditions of the beam pumping unit [2] but also calculates the balance of the pumping unit, reducer output shaft torque, and motor power [3, 4]. At the same time, the actual polished rod dynamometer card can be matched with the fault cards, which are often used to diagnose the fault of the oil well [5–11]. Thus, it is very meaningful to study the polished rod load.

First, the approximate formula was used to calculate the polished rod load of pumping units. For example, only the gravity of the rod string in the air and the buoyancy of liquid to the rod string were considered. The most common method is the API method [12] published by the American Petroleum Institute. The results of the method were compared with the results measured from 77 wells in the field, and the results are relatively accurate. In 1963, Gibbs [13] introduced the prediction model of the sucker rod pumping system, which laid the theoretical foundations for the accurate design of sucker rod pumping systems. A one-dimensional wave equation with damping was established in the prediction model, along with the boundary conditions and initial conditions of the rod and pump. The finite difference method was used to solve the wave equation, and the rod dynamometer card in any section can be drawn accurately. Later, Gibbs [14] summarized the methods for the design and analysis of rod pumping installations and applied the wave equation to the fault diagnosis of the sucker rod pumping system. In 1983, Doty and Schmidt [15] presented a two-dimensional model for predicting the

behavior of sucker rod pumping installations. The model considered the dynamics of the fluid and tubing columns as well as the physical properties of the fluid. This provided a new way of analyzing the effects of fluid properties on a sucker rod pumping installation. In 1992, Wang et al. [16] proposed the three-dimensional vibration of the sucker rod, tubing, and liquid column in the sucker rod pumping system. The results indicated that the new model is an improvement over existing one-dimensional and two-dimensional models.

Since the twentieth century, studies on polished rod load have focused on two aspects. The first is a new research object. In order to reduce the polished rod load, Luan et al. [17] presented a side-flow pump, which offered the possibility of deeper setting depth of the pump in oil wells and could be used in deep well sucker rod pumping. Rotaflex is a completely mechanical long-stroke pumping unit. For the first time, Takacs [18] conducted a thorough investigation of the kinematic performance of Rotaflex pumping units and developed exact formulas for the calculation of polished rod position, velocity, acceleration, and load. According to the demand for offshore heavy oil thermal recovery and the production of stripper wells, Yu et al. [19] designed a new miniature hydraulic pumping unit with long stroke, low pumping speed, and compact structure to resolve the problem of limited space. Through the establishment of the mechanical model for rods, the polished rod load was calculated. The smooth operation of the prototype verified the practicality and effectiveness of the overall design scheme and laid the foundations for field testing. Recently, Liu et al. [20–22] conducted a series of experiments on a coalbed methane (CBM) well. A modern methodology was proposed for the system design of dynamic behavior to conduct accurate and pertinent analysis of CBM pumping installations. Through the establishment of the model, the polished rod load was accurately predicted. The second aspect is a new research method. Gong et al. [23] proposed a predictive algorithm based on a least squares support vector machine model and applied it to oil pumping wells. Li et al. [24] established a coupled dynamic model for describing the dynamic performance of the polished rod load of beam pumping units. The oilfield application showed the effectiveness and accuracy of the new model, which could be used to predict operating parameters such as load, pump efficiency, torque, and balance, as well as in-fault diagnosis. Feng et al. [25] developed a set of rated power calculation methods and a set of matching templates with the intention of improving the efficiency of the prime motor and decreasing the cost of rod pumping. The tested data showed that the polished rod load decreased substantially. Chen et al. [26] developed an optimal control approach for predicting the behavior of sucker rod pumping systems. The method provided error correction in predictions and generated accurate polished rod and intermediate-depth work dynagraphs for any bottom-hole pump condition in vertical oil wells.

In the actual pumping process, wear develops between the plunger and pump barrel of the oil pump, but previous prediction models failed to consider the effects of wear. In the vibration model of the rod string, the real factors that influence the downstroke boundary conditions have also increased. Therefore, a wear model between the plunger and pump barrel is established, and the wear mechanism between the plunger and pump barrel is studied. The wave equation of the sucker rod string is developed, and the upper and downhole boundary conditions are determined as well as the initial conditions. Taking the clearance between the plunger and pump barrel as a parameter, the effects of clearance caused by wear on the polished rod dynamometer card is analyzed.

2. Wear Modeling of Plunger-Pump Barrel

The wear of friction pairs in the plunger-pump barrel will cause the failure of the sucker rod pumping system, a process that involves adhesive wear, abrasive wear, and corrosion wear. Since the system is assembled with clearance between the plunger and pump barrel, the presence of crude oil in the clearance between the plunger and pump barrel acts as a lubricant. The wear of plunger-pump barrel increases with high sand content, high water content, and *incorrect* combination of the plunger and pump barrel in the oilfield. Specifically, a large amount of sand will enter the wedge clearance with increasing the sand content, and the surfaces of the plunger and pump barrel are vulnerable to wear. The lubrication performance of oil-water mixtures is greatly reduced with increasing water content. The coefficient of friction between the plunger and pump barrel also increases, which accelerates the wear of the plunger. When the clearance is too small, adhesive wear occurs on the contact surfaces of the plunger and pump barrel owing to the lack of lubrication. In addition, corrosion occurs at the contact surfaces between the plunger and pump barrel in acid, alkali, salt, and other special medium. Bu [27] pointed out that the main component of pump wear was sand. Therefore, the wear type between the plunger and pump barrel is identified only as abrasive wear in this study.

In order to facilitate the establishment of the wear model, the following assumptions are made:

(1) It is assumed that wear only occurs on the pump barrel, instead of the plunger and abrasive.

(2) The radial load of abrasive particles from the pump barrel is defined as the average value of radial loads on the upstroke and downstroke.

(3) The abrasive particle is spherical with a specific diameter. When the clearance between the plunger and pump barrel is larger than the diameter of the abrasive particle, the abrasive particle falling into the pump will not cause wear on the barrel. Larger abrasive particles continue to wear on the pump barrel and the wear process will continue the wear limit is reached.

It is assumed that the diameter of the first abrasive particle is D_1, the diameter of the second one is D_2, and the diameter of the nth one is D_n. Therefore,

$$D_1 - \delta_1 = D_2 - D_1 = \ldots = D_n - D_{n-1} = \delta, \quad (1)$$

where δ_1 is the initial fit clearance of the plunger and pump barrel, δ is the radial wear depth of the abrasive particle, and $\delta = 10^{-2}\delta_1$.

Taking a single abrasive particle as the object of study, mechanical analysis of the abrasive particle was carried out during the upstroke and downstroke, which are shown in Figures 1 and 2. Based on the mechanical analysis, the mechanical models of the abrasive particle are established.

In Figures 1 and 2, N_{Bu} and N_{Bd} are the radial forces of the pump barrel, N_{pu} and N_{pd} are the support forces of the plunger, F_{Bu} and F_{Bd} are the friction of the pump barrel, and F_{Pu} and F_{Pd} are the friction of the plunger on the upstroke and downstroke. G is the gravity of the abrasive particle, and θ is the angle between the plumb line and chamfer surface of the plunger. Combined with the forces acting on the abrasive particle in Figures 1 and 2, the following equations can be obtained.

On the upstroke,

$$\begin{aligned} N_{Bu} - N_{Pu}\cos\theta + F_{Pu}\sin\theta = 0, \\ N_{Pu}\sin\theta + F_{Pu}\cos\theta - F_{Bu} - G = 0. \end{aligned} \tag{2}$$

On the downstroke,

$$\begin{aligned} N_{Bd} - N_{Pd}\cos\theta - F_{Pd}\sin\theta = 0, \\ N_{Pd}\sin\theta + F_{Pd}\cos\theta - F_{Bd} - G = 0. \end{aligned} \tag{3}$$

In Equations (2) and (3), the friction force is equal to the pressure multiplied by the friction coefficient. This means that $F_{Bu} = \mu \cdot N_{Bu}$, $F_{Bd} = \mu \cdot N_{Bd}$, $F_{Pu} = \mu \cdot N_{Pu}$, and $F_{Pd} = \mu \cdot N_{Pd}$, where μ is the friction coefficient. It is obvious that N_{Bu} and N_{Bd} can be determined by simplifying Equations (2) and (3).

Based on the energy wear theory [28], the computational model for determining the wear volume of the pump barrel under the action of the i-th abrasive particle is established as follows:

$$V_i = \frac{Q}{H} P_i L_i, \tag{4}$$

where Q is the coefficient of wear, H is the Brinell hardness of pump barrel material, L_i is the friction distance of the i-th abrasive particle to the pump barrel, and P_i is the radial force of the i-th abrasive particle to the pump barrel.

According to the model assumptions, the radial force of the i-th abrasive particle to the pump barrel is calculated by the following formula:

$$P_i = \frac{N_{Bu(i)} + N_{Bd(i)}}{2}, \tag{5}$$

where $N_{Bu(i)}$ and $N_{Bd(i)}$ are the values of N_{Bu} and N_{Bd} at the i-th abrasive particle.

In Equation (4), Q and H are known in the calculation process. In order to study L_i, the wear volume V_i should be calculated first. According to the actual wear condition of the pump barrel, the geometric model of abrasive wear between plunger and pump barrel is established, as shown in Figure 3.

As can be seen in Figure 3, the area of the AECD is the wear area of the abrasive particle and pump barrel. The key to calculating the wear volume is to acquire the area of the AECD. According to the geometric relationship, the area

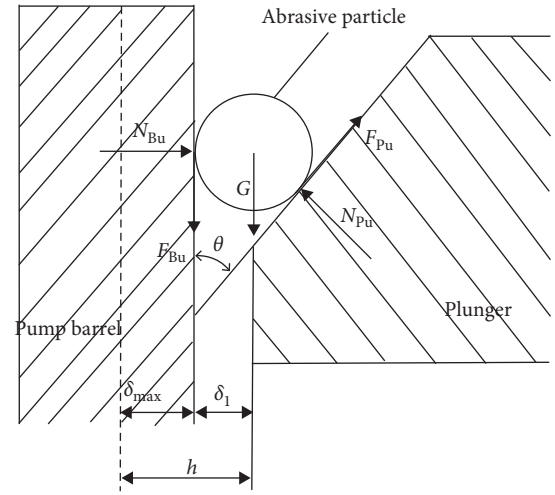

Figure 1: The forces of the abrasive particle on upstroke.

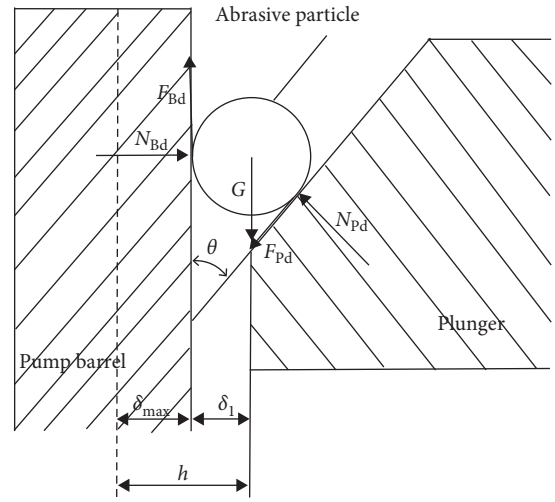

Figure 2: The forces of the abrasive particle on downstroke.

of AECD can be obtained as shown in the following equation:

$$\begin{aligned} S_{AECD} &= S_{O_1ADC} - S_{O_1AEC} = S_{O_1ADC} - S_{O_1ABC} - S_{ABEC} \\ &= S_{O_1ADC} - S_{O_1ABC} - S_{OAEC} + S_{OABC}, \end{aligned} \tag{6}$$

where S denotes the area.

For the i-th abrasive particle, O_1ADC and $OAEC$ are sectors while O_1ABC and $OABC$ are triangles. According to the corresponding area calculation formula, the areas of O_1ADC, $OAEC$, O_1ABC, and $OABC$ are calculated. Using Equation (6), the wear area of the i-th abrasive particle S_i can be obtained. As the pump is a reciprocating mechanism, the wear volume of the pump barrel is equal to the wear area multiplied by the pump stroke. That is $V_i = s \cdot S_i$, where s is the pump stroke.

In Equation (4), L_i is a function of time, which is written as

$$L_i = 2.88 \times 10^3 sNT_i, \tag{7}$$

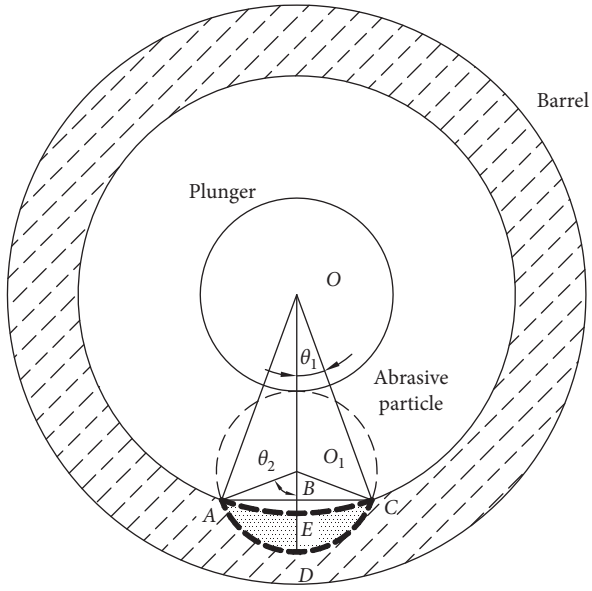

Figure 3: The geometric model of abrasive wear.

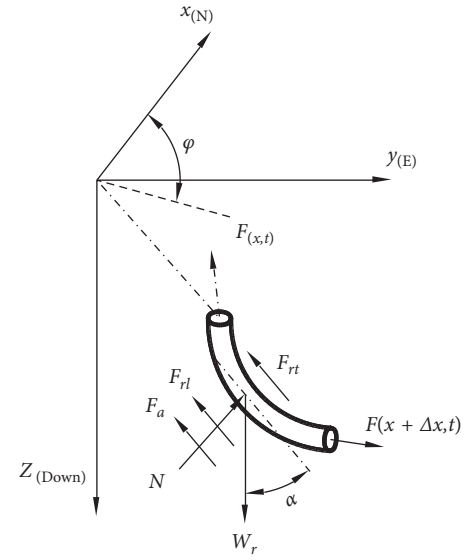

Figure 4: Force schematic diagram of the sucker rod microunit.

where N is the pump speed and T_i is the wear time of the i-th abrasive particle. Therefore, according to Equations (4) and (7), the wear time of the i-th abrasive particle can be obtained.

3. Vibration Modeling of the Rod String

3.1. Mechanical Analysis of the Rod String. In order to analyze the forces of the sucker rod, the microunit of the sucker rod is taken as a research object. The forces of the microunit include the axial force of the microunit acting on the upper cross section and lower cross section ($F(x,t)$ and $F(x_{+\Delta}x,t)$), the inertia force of the microunit (F_a), the viscous force and support reaction force acting on the microunit (F_{rl} and N), the frictional force between the tubing and sucker rod (F_{rt}), and gravity of the sucker rod (W_r). The forces are applied as shown in Figure 4.

The mechanical analysis process is simplified and the wave equation of the sucker rod is obtained by referring to previous study [29].

$$\frac{\partial^2 u}{\partial t^2} = a^2 \frac{\partial^2 u}{\partial x^2} - c\frac{\partial u}{\partial t} - \delta h N + g' \cos\theta, \tag{8}$$

where $a = \sqrt{E_r/\rho_r}$, $c = \nu_e/\rho_r A_r$, $h = f/\rho_r A_r$, and $g' = \rho_r' g/\rho_r$.

In Equation (8), $u(x,t)$ is the displacement along the depth direction in position x of the sucker rod at time t. E_r is the modulus of elasticity of the sucker rod, and ρ_r is sucker rod density. ν_e is the viscous damping coefficient per unit length of the sucker rod, and A_r is the cross-sectional area of the sucker rod. δ determines the direction of the force, and is equal to -1 if the sucker rod is operating on the upstroke; otherwise it is equal to $+1$. f is the friction coefficient between the tubing and sucker rod. N is the support reaction force acting on the microunit from the tubing. ρ_r' is the relative density of the sucker rod in oil, and g is the acceleration of gravity.

3.2. Upper Boundary Condition. In order to solve the wave equation of the sucker rod, the upper boundary condition needs to be given first. In fact, the upper boundary condition is the upper endpoint movement of the sucker rod, which is the same as the displacement of the polished rod. That is

$$u(0,t) = U_0, \tag{9}$$

where $u(0,t)$ is the value of $u(x,t)$ at $x = 0$ and U_0 is the polished rod displacement.

The displacement of the polished rod was obtained by studying the motion law of the pumping unit. In one pumping process, the rotation of the crank leads the movement of the walking beam, which drives horse head moving from the down-fixed point to the up-fixed point, and then moving to the down-fixed point. Figure 5 is a sketch of the mechanism of the conventional beam pumping unit. It can be seen that ψ is the angle between C and K, where C is the back-arm length of the beam and K is the distance between the support center of the beam and the output shaft center of the gear reducer. When the horse head is at the down-fixed point, the angle ψ is defined as ψ_b. When the horse head is at the up-fixed point, the angle ψ is defined as ψ_t. According to the triangle cosine theorem, these two angles can be obtained

$$\begin{aligned} \psi_b &= \arccos\left(\frac{C^2 + K^2 - (P+R)^2}{2CK}\right), \\ \psi_t &= \arccos\left(\frac{C^2 + K^2 - (P-R)^2}{2CK}\right), \end{aligned} \tag{10}$$

where P is the length of pitman arm and R is the radius of the crank.

Therefore, the calculation formula of the polished rod displacement of the pumping unit can be given as

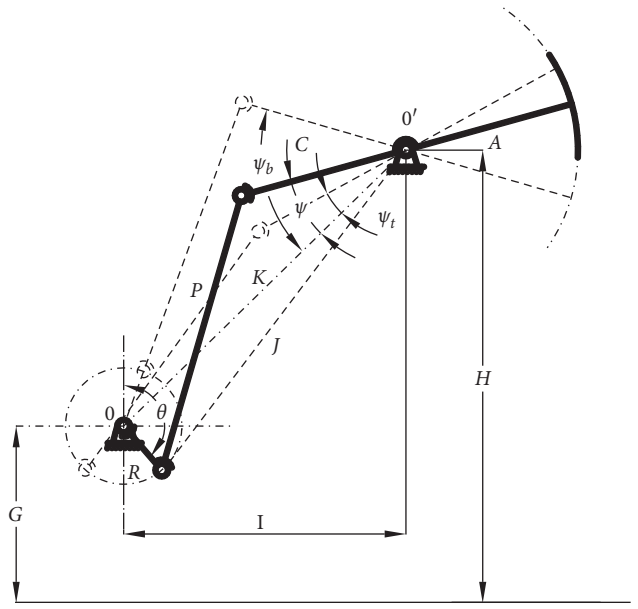

Figure 5: Sketch of the mechanism of the conventional beam pumping unit.

$$U_0 = \frac{\psi_b - \psi}{\psi_b - \psi_t} s, \tag{11}$$

where s is the polished rod stroke. After determining the type of the pumping unit, the geometric parameters of the pumping unit are obtained. Substituting the values of ψ_t and ψ_b calculated by geometric parameters in Equation (11), the polished rod displacement of the pumping unit is obtained.

3.3. Downhole Boundary Conditions. The downhole boundary conditions refer to the relationship between the load acting on the plunger and plunger displacement. The downhole boundary conditions [29] can be written as follows:

$$\alpha u(L,t) + \beta \frac{\partial u(L,t)}{\partial x} + \gamma \frac{\partial^2 u(L,t)}{\partial t^2} + \kappa \frac{\partial u(L,t)}{\partial t} = p(t). \tag{12}$$

In Equation (12), the second term represents the liquid load acting on the plunger on upstroke. The third term represents the liquid inertial load acting on the upper part of the plunger on upstroke. When the plunger is in the acceleration section of upstroke, γ is the liquid mass on the upper part of the plunger. When the plunger is in the deceleration section of upstroke or downstroke, γ is equal to zero. The fourth term represents the frictional force between the plunger and pump barrel. The κ in the formula is determined by the following expression:

$$\kappa = 2\pi\mu L_{\mathrm{p}} \ln\left(\frac{R_{\mathrm{p}}}{R_{\mathrm{b}}}\right), \tag{13}$$

where μ is the dynamic viscosity of the well liquid and L_{p}, R_{p}, and R_{b} are the plunger length, plunger radius, and barrel, respectively.

In actual production, when the oil pump is in different stages, the values of α, β, and $p(t)$ are different. By judging the opening and closing of the standing valve and traveling valve in the oil pump, the values of α, β, and $p(t)$ are determined, and the downhole boundary conditions of the sucker rod pumping system are calculated.

3.4. Initial Conditions. When solving Equation (8), the initial condition must first be given. As the vibration of the sucker rod string is forced vibration with damping, it can assume any initial condition. In order to facilitate the simulation of downhole boundary conditions, the following initial conditions can be adopted. Assuming that the electric motor starts at $t = 0$, the polished rod is at the down-fixed point. At $t = 0$, the whole sucker rod string is at the stationary state, which means that

$$\begin{aligned} u(x,0) &= 0, \\ u'(x,0) &= 0, \end{aligned} \tag{14}$$

where $u(x, 0)$ is the value of $u(x, t)$ at $t = 0$ and $u'(x, 0)$ is the partial derivative value of $u(x, t)$ to t at $t = 0$.

4. The Establishment of a Mixed Difference Scheme

In this study, the finite difference method was used to approximate Equation (8). The calculation process of explicit difference is simple, but the convergence condition is strong. For the purpose of overcoming the limitations of the convergence condition and speed using the explicit difference format, the implicit difference format was chosen to approximate Equation (8). Owing to the complex and changeable underground structure, a multistage rod was used for oil recovery. When an equal step difference is used to establish a difference scheme for the multistage rod, the density, elastic modulus, etc., need to be homogenized first. As the ratios of various types of sucker rods are uncertain, the accuracy of the calculation is difficult to guarantee. In order to overcome the above shortcomings, the multistage rod is considered as multiple homogeneous rods. A three-storey implicit difference format was adopted for the homogeneous rod, and variable step-length difference was adopted between different adjacent homogeneous rods.

4.1. Difference Scheme of Homogeneous Rod. In the homogeneous rod, Δx is selected as the node of equal step along the axial direction of the sucker rod. Then, the sucker rod is divided into m units, and i is the subscript notation, $i = 1, 2, \ldots, m$. Δt was selected as the node of equal step along the time direction, and j is the subscript notation, $j = 1, 2, \ldots, n$. Thus, $u_{i,j}$ represents the i node displacement of the rod string at j time.

In the node (i, j), central difference quotient formulas were selected to approximate $\partial u/\partial t$ and $\partial^2 u/\partial t^2$, which means that

$$\left(\frac{\partial u}{\partial t}\right)_{i,j} = \frac{u_{i,j+1} - u_{i,j-1}}{\Delta t}, \tag{15}$$

$$\left(\frac{\partial^2 u}{\partial t^2}\right)_{i,j} = \frac{u_{i,j+1} + u_{i,j-1} - 2u_{i,j}}{\Delta t^2}. \tag{16}$$

Furthermore, the weighted average formula of central difference quotient in j–1, j, and j+1 layers was chosen to approximate $\partial^2 u/\partial x^2$

$$\begin{aligned}\left(\frac{\partial^2 u}{\partial x^2}\right)_{i,j} &= \eta \frac{u_{i+1,j+1} + u_{i-1,j+1} - 2u_{i,j+1}}{\Delta x^2} \\ &+ (1 - 2\eta) \frac{u_{i+1,j} + u_{i-1,j} - 2u_{i,j}}{\Delta x^2} \\ &+ \eta \frac{u_{i+1,j-1} + u_{i-1,j-1} - 2u_{i,j-1}}{\Delta x^2},\end{aligned} \tag{17}$$

where η is the weighted coefficient. In order to facilitate the calculation, it is defined that $\eta = 1/2$.

By combining Equations (15)–(17) with (8), Equation (8) can be simplified as

$$\begin{aligned}&-\frac{a^2}{4\Delta x^2} u_{i-1,j+1} + \left(\frac{a^2}{2\Delta x^2} - \frac{c}{2\Delta t} - \frac{1}{\Delta t^2}\right) u_{i,j+1} + \frac{a^2}{4\Delta x^2} u_{i+1,j+1} \\ &= 2a_1\left(u_{i+1,j} - u_{i-1,j}\right) + a_2 u_{i,j} + a_1\left(u_{i+1,j-1} - u_{i-1,j-1}\right) \\ &\quad + a_3 u_{i,j-1} - b_{i,j},\end{aligned} \tag{18}$$

where

$$\begin{aligned}a_1 &= -\frac{a^2}{4\Delta x^2}, \\ a_2 &= -\frac{a^2}{\Delta x^2} + \frac{2}{\Delta t^2}, \\ a_3 &= -\frac{a^2}{\Delta x^2} - \frac{c}{2\Delta t}, \\ b_{i,j} &= \delta_{i,j} h_i N_{i,j} - g_j' \cos\theta.\end{aligned} \tag{19}$$

In Equation (18), $u_{i-1,j+1}$, $u_{i,j+1}$, and $u_{i+1,j+1}$ on the left side of the equal sign are unknown quantities that need to be solved by simultaneous equations. This is a three-storey implicit difference format, as shown in Figure 6.

4.2. Difference Scheme of the Connection between Two Homogeneous Rods. A two-stage rod was selected as an example. Δx_1 is defined as the axial step of the first homogeneous rod, while Δx_2 is defined as the axial step of the second homogeneous rod, as shown in Figure 7. According to Equation (8), the wave equations of two different homogeneous rods can be obtained

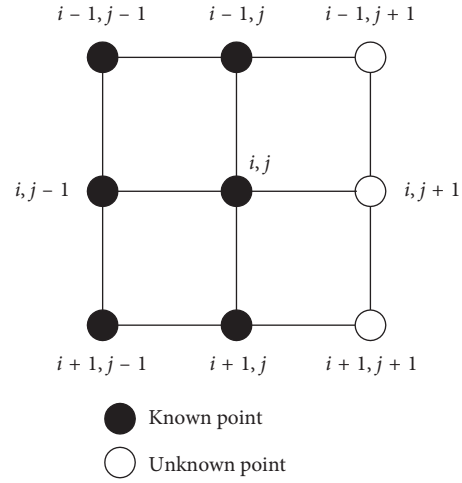

Figure 6: Three-storey implicit difference format.

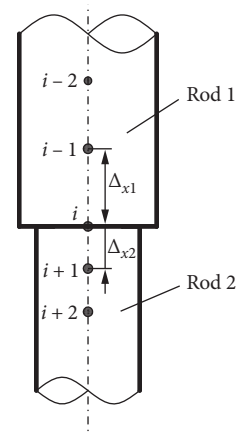

Figure 7: Sketch map of sucker rod interface.

$$\frac{\partial^2 u}{\partial t^2} = a_l^2 \frac{\partial^2 u}{\partial x^2} - c_l \frac{\partial u}{\partial t} - \delta h_l N + g_l' \cos\theta, \tag{20}$$

where l is equal to 1 or 2.

In Figure 7, the differential formats of the wave equations in each node are the same as Equation (18) except node i. In node i, the continuity conditions of force $F(i, j)$ and displacement $u(i, j)$ should be satisfied. That is

$$F(i, j)_1 = F(i, j)_2 \cdot u(i, j)_1 = u(i, j)_2. \tag{21}$$

Then, Equation (21) is combined with the Taylor formula to obtain

$$\left(\frac{\partial u}{\partial x}\right)_{i1} = \frac{u_{i,j} - u_{i-1,j}}{\Delta x_1} + \left(\frac{\partial^2 u}{\partial x^2}\right)_{i1} \frac{1}{2} \Delta x_1, \tag{22}$$

$$\left(\frac{\partial u}{\partial x}\right)_{i2} = \frac{u_{i+1,j} - u_{i,j}}{\Delta x_2} + \left(\frac{\partial^2 u}{\partial x^2}\right)_{i2} \frac{1}{2} \Delta x_2. \tag{23}$$

With the combination of Equations (20) to (23), the difference equation of different materials in the connection of different diameter rods is expressed by

$$u_{i,j+1} = \frac{(2b_1 + b_2 - v_2 - v_1) - b_1 u_{i,j} + v_2 u_{i+1,j} + v_1 u_{i-1,j}}{b_1 + b_2} - \frac{r_1\left(\delta_{i,j} h_{1i} N_{i,j} - g'_{1j}\cos\theta_i\right) + r_2\left(\delta_{i,j} h_{2i} N_{i,j} - g'_{1j}\cos\theta_i\right)}{b_1 + b_2}, \tag{24}$$

where

$$b_1 = \frac{(\Delta x E_r A_r)_1}{2(a_1\Delta t)^2} + \frac{(\Delta x E_r A_r)_2}{2(a_2\Delta t)^2},$$
$$b_2 = \frac{(\Delta x E_r A_r c)_1}{2a_1^2\Delta t} + \frac{(\Delta x E_r A_r c)_2}{2a_2^2\Delta t},$$
$$r_i = \frac{(\Delta x E_r A_r)_i}{2a_1^2}, \tag{25}$$
$$v_i = \frac{(E_r A_r)_i}{\Delta x_i}, \quad i = 1, 2,$$

5. Instance Calculation and Analysis

In order to investigate the true wear condition between the plunger and pump barrel, an example is given. The simulation parameters are listed in Table 1. By substituting the parameters in Table 1 in Equation (6), the wear area of a single abrasive is calculated, and then the wear volume of a single abrasive can be obtained, as shown in Figure 8.

Figure 8 shows the variation of wear volume with abrasive diameter. In Figure 8, the wear volume of each abrasive increases with the increase in abrasive diameter. Further observation of the wear volume curve in Figure 8 shows that the slope of the wear volume curve increases with the increase in abrasive diameter. This indicates that the wear volume rate increases with the abrasive diameter.

Taking the calculated wear volume into Equation (4), the abrasive wear distance L_i can be obtained. Using Equation (7), the wear time of a single abrasive particle is achieved, as shown in Figure 9.

Figure 9 describes the change curves of wear time with particle diameter under different θ, where θ is the angle between the plumb line and chamfer surface of the plunger. From Figure 9, it is found that the wear times of three different θ always increase with the increase in abrasive diameter. Further observation of Figure 9 shows that the slope of the wear time curve decreases with the increase in abrasive diameter, which indicates that the rate of increase of wear time decreases with the increase in abrasive diameter. Comparison of the three curves shows that the increase of θ extends the wear time of each abrasive.

With the increase in wear time, the increase in wear depth affects the change of clearance of the plunger and pump barrel. To further discuss the influence of wear on the sucker rod pumping system, the clearance of the plunger and pump barrel was selected as a parameter, i.e., δ. Well L2111 in the Liao He Oilfield was selected for the experiments. Tables 2 and 3 list the relevant parameters of the pumping unit, sucker rod, oil pump, and tubing, respectively. In Table 2, A represents beam front arm length, C represents beam rear arm length, P represents the length of pitman arm, G represents the height from the center of the speed reducer output shaft, H represents the height from beam support center to the bottom of the pedestal, I represents the horizontal distance between beam support center and the center of the speed reducer output shaft, and R represents the radius of the crank.

According to the parameter data of the pump unit in Table 2, the polished rod displacement curve can be achieved by solving Equation (11), as shown in Figure 10. By determining the surface boundary conditions of the polished rod displacement, the wave equation can be solved, and the polished rod load of sucker rod pumping system can be obtained.

Figure 11 describes the variation trend of polished rod load with δ in well L2111, where δ is the clearance of the plunger and pump barrel. To better illustrate the effect of wear on the system, three different values of δ were considered. It can be seen that δ influences the polished rod load. Comparison of the three curves in Figure 11 shows that there is an obvious decrease in polished rod load with the increase of δ on the upstroke. This is because with increasing pumping time, the wear depth between the plunger and pump barrel increases. The increase of δ will lead to an increase in leakage between the plunger and pump barrel, which will reduce lifting oil production and polished rod load. At the same time, with the increase of δ, the influence of δ on load gradually decreases. On the downstroke, the influence of δ changes on the polished rod load is very small. This is because the traveling valve is open, and oil is flowing in the pump. No liquid column loading was found on the plunger. In the whole pumping process, the changes in δ caused by wear between the plunger and pump barrel will affect the change in polished rod dynamometer cards of the sucker rod pumping system, which cannot be ignored.

6. Conclusion

(1) In order to study the influence of wear between the plunger and pump barrel of the oil pump on the polished rod dynamometer card, the wear model of the plunger-pump barrel was established. On the basis of considering abrasive wear, the forces on the abrasive particle were analyzed. By calculating the wear area of abrasive particles, the change curves of wear volume and wear time versus abrasive particle diameter were obtained.

(2) The wave equation of the sucker rod string from a previous study was selected, and the upper boundary condition, downhole boundary condition, and initial condition were determined. A three-storey implicit difference format was applied to the homogeneous rod while the variable step-length

Table 1: Simulation parameters of wear.

The parameter name	Values	The parameter name	Values	The parameter name	Values
Pump stroke	3.54 (m)	Pump speed	2.45 (min^{-1})	Pump diameter	44 (mm)
Wear coefficient	6.5	Dynamic friction coefficient	0.145	Abrasive density	2560 (kg/m^3)
Pump barrel hardness	280 (N/mm^2)	Initial clearance	0.05 (mm)	Clearance increment	0.0005 (mm)

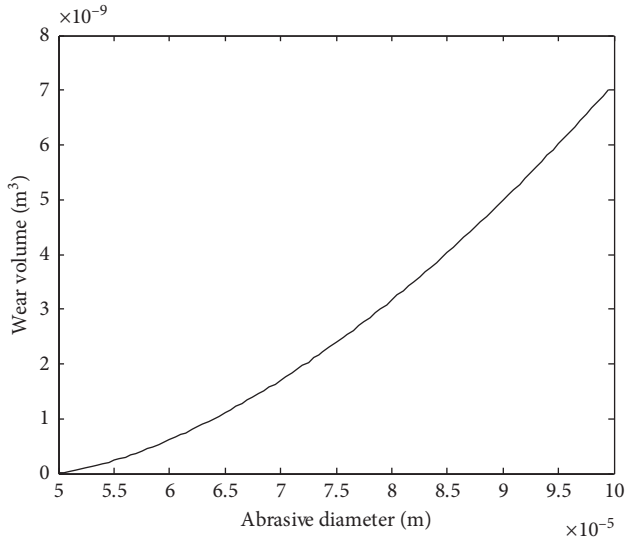

Figure 8: Wear volume change curve.

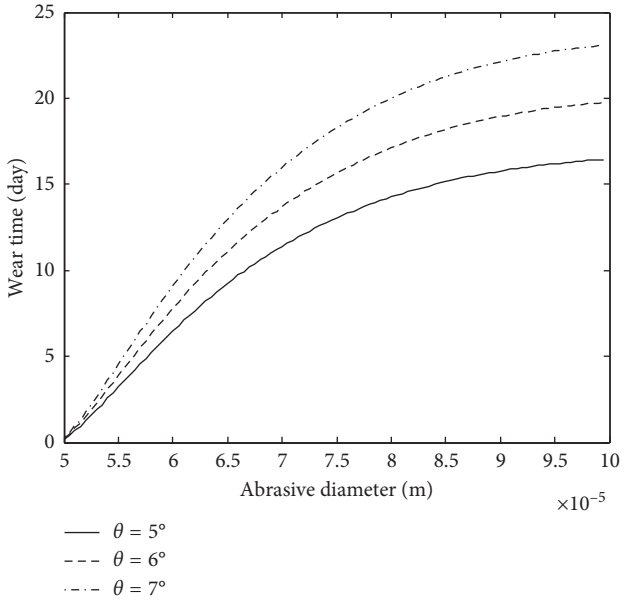

Figure 9: Wear time change curves.

difference format was adopted between adjacent different homogeneous rods. Finally, the wave equation was solved by the mixed finite difference method.

(3) In order to discuss the influence of wear on the polished rod dynamometer card, a well from the Liao He Oilfield was used for the experiment. The polished rod dynamometer card shows that the increase in clearance between the plunger and pump barrel leads to a decrease in polished rod load on upstroke. In view of the influence of clearance on the polished rod dynamometer card, it is meaningful to study the sucker rod pumping system by considering the wear between the plunger and pump barrel.

Table 2: Equipment parameters of pump unit, pump, and tubing.

The parameter name	Values	The parameter name	Values	The parameter name	Values
Pump stroke	3.54 (m)	Pump speed	2.45 (min^{-1})	A	4.81 (m)
C	2.906 (m)	P	4 (m)	G	2 (m)
H	6 (m)	I	7 (m)	R	1.04 (m)
Pump diameter	ϕ44 (mm)	Pump depth	1997 (m)	Plunger area	11.34×10^{-4} (m^2)
Cross-sectional area of tubing	5.6×10^{-4} (m^2)	Flow area of tubing	12.8×10^{-4} (m^2)	Elastic constant of tubing	8.67×10^{-6} $(kN)^{-1}$

Table 3: Equipment parameters of sucker rod.

Sucker rod diameter	Length	Cross-sectional area	Deadweight	Elastic constant
ϕ19 mm	710 m	2.84×10^{-4} m^2	2.35×10^{-2} kN/m	1.664×10^{-5} $(kN)^{-1}$
ϕ22 mm	890 m	3.80×10^{-4} m^2	3.14×10^{-2} kN/m	1.241×10^{-5} $(kN)^{-1}$
ϕ25 mm	174 m	4.91×10^{-4} m^2	4.09×10^{-2} kN/m	0.961×10^{-5} $(kN)^{-1}$

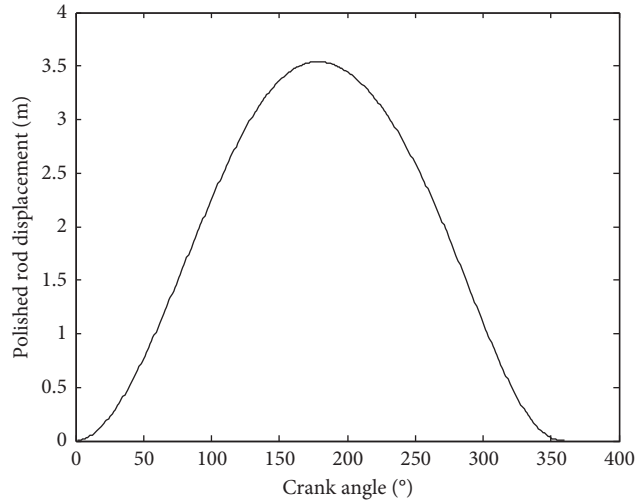

Figure 10: The displacement curve of polished rod.

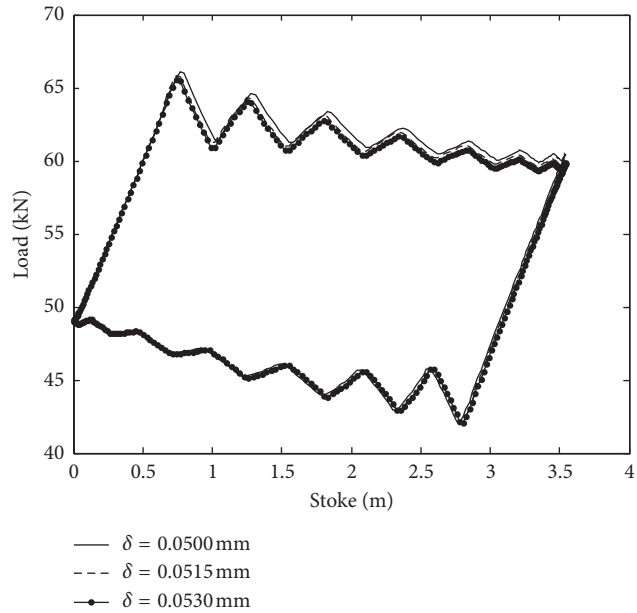

Figure 11: Polished rod dynamometer cards of well L2111.

Data Availability

The parameters required in the simulation and experiment are given in Tables 1, 2, and 3 in the article or can be obtained from the corresponding author upon request.

Conflicts of Interest

The authors declare that they have no conflicts of interest.

Acknowledgments

The financial supports of National Natural Science Foundation of China (51275404) and Shaanxi 13115 Major R&D Project (2009ZDKG-33), and data support of Liao He Oilfield are gratefully acknowledged.

References

[1] W. Du, "Observations of China's oil industry in the 13th five-year plan period," *International Petroleum Economics*, vol. 25, no. 4, pp. 28–32, 2017, in Chinese.

[2] K. Li, Y. Han, and T. Wang, "A novel prediction method for down-hole working conditions of the beam pumping unit based on 8-directions chain codes and online sequential extreme learning machine," *Journal of Petroleum Science and Engineering*, vol. 160, pp. 285–301, 2018.

[3] H. J. Meng, L. Quan, Z. L. Wang, C. W. Wang, and Y. Lan, "An energy-saving pumping system with novel springs energy storage devices: design, modeling, and experiment," *Advances in Mechanical Engineering*, vol. 9, no. 1, pp. 1–11, 2017.

[4] K. Li and Y. Han, "Modelling for motor load torque with dynamic load changes of beam pumping units based on a serial hybrid model," *Transactions of the Institute of Measurement and Control*, vol. 40, no. 3, pp. 903–917, 2018.

[5] K. Wang, "Modeling method for fault diagnosis to sucker rod pumping system in directional well," *Journal of China University of Petroleum*, vol. 34, no. 2, pp. 130–135, 2010, in Chinese.

[6] M. M. Xing, S. M. Dong, Z. X. Tong, R. F. Ran, and H. L. Chen, "Dynamic simulation and efficiency analysis of beam pumping system," *Journal of Central South University*, vol. 22, no. 9, pp. 3367–3379, 2015.

[7] K. Li, X. W. Gao, H. B. Zhou, and Y. Han, "Fault diagnosis for down-hole conditions of sucker rod pumping systems based on the FBH-SC method," *Petroleum Science*, vol. 12, no. 1, pp. 135–147, 2015.

[8] L. M. Lao and H. Zhou, "Application and effect of buoyancy on sucker rod string dynamics," *Journal of Petroleum Science & Engineering*, vol. 146, pp. 264–271, 2016.

[9] T. Ren, X. Q. Kang, W. Sun, and H. Song, "Study of dynamometer cards identification based on root-mean-square error algorithm," *International Journal of Pattern Recognition & Artificial Intelligence*, vol. 32, no. 2, article 1850004, 2017.

[10] B. Y. Zheng and X. W. Gao, "Sucker rod pumping diagnosis using valve working position and parameter optimal continuous hidden Markov model," *Journal of Process Control*, vol. 59, pp. 1–12, 2017.

[11] A. Zhang and X. W. Gao, "Fault diagnosis of sucker rod pumping systems based on Curvelet Transform and sparse multi-graph regularized extreme learning machine," *International Journal of Computational Intelligence Systems*, vol. 11, no. 1, pp. 428–437, 2018.

[12] X. M. Wu and X. R. Wang, "Mathematical simulation of calculation chart for oil pumping rod load," in *Proceedings of Asia-Pacific Conference on Information Processing*, vol. 2, pp. 407–409, IEEE Computer Society, Shenzhen, China, 2009.

[13] S. G. Gibbs, "Predicting the behavior of sucker-rod pumping systems," *Journal of Petroleum Technology*, vol. 15, no. 7, pp. 769–778, 1963.

[14] S. G. Gibbs, "A review of methods for design and analysis of rod pumping installations," *Journal of Petroleum Technology*, vol. 34, no. 12, pp. 2931–2940, 1982.

[15] D. R. Doty and Z. Schmidt, "An improved model for sucker rod pumping," *Society of Petroleum Engineers Journal*, vol. 23, no. 1, pp. 33–41, 1983.

[16] G. W. Wang, S. S. Rahman, and G. Y. Yang, "An improved model for the sucker rod pumping system," in *Proceedings of 11th Australasian Fluid Mechanics Conference*, pp. 1137–1140, Australasian Fluid Mechanics Society, Hobart, Australia, 1992.

[17] G. H. Luan, S. L. He, and Z. Yang, "A prediction model for a new deep-rod pumping system," *Journal of Petroleum Science and Engineering*, vol. 80, no. 1, pp. 75–80, 2012.

[18] G. Takacs, "Exact kinematic and torsional analysis of rotaflex pumping units," *Journal of Petroleum Science and Engineering*, vol. 115, no. 3, pp. 11–16, 2014.

[19] Y. Q. Yu, Z. Y. Chang, Y. G. Qi, X. Xue, and J. N. Zhao, "Study of a new hydraulic pumping unit based on the offshore platform," *Energy Science & Engineering*, vol. 4, no. 5, pp. 352–360, 2016.

[20] X. F. Liu and Y. G. Qi, "A modern approach to the selection of sucker rod pumping systems in CBM wells," *Journal of Petroleum Science and Engineering*, vol. 76, no. 3, pp. 100–108, 2011.

[21] X. F. Liu, "Prediction of flowing bottomhole pressures for two-phase coalbed methane wells," *Acta Geologica Sinica-English Edition*, vol. 87, no. 5, pp. 1412–1420, 2013.

[22] X. F. Liu, C. H. Liu, and Y. Yang, "Dynamic behavior of the polished rod for the coalbed methane pumping installations," *Oil & Gas Science and Technology*, vol. 72, no. 3, p. 16, 2017.

[23] R. B. Gong, W. R. Zhu, and J. Y. Ding, "Trend Prediction of indicator diagram based on least squares support vector machines," *Petroleum Planning & Engineering*, vol. 26, no. 4, pp. 24–27, 2015, in Chinese.

[24] X. Y. Li, X. W. Gao, Y. B. Hou, and H. R. Wang, "Coupled dynamic modeling for polished rod load of beam pumping unit," *Journal of Northeastern University (Natural Science)*, vol. 37, no. 9, pp. 1225–1229, 2016, in Chinese.

[25] Z. M. Feng, J. J. Tan, X. L. Liu, and F. Xin, "Selection method modelling and matching rule for rated power of prime motor used by beam pumping units," *Journal of Petroleum Science and Engineering*, vol. 153, pp. 197–202, 2017.

[26] Z. S. Chen, L. W. White, and H. M. Zhang, "Predicting behavior of sucker-rod pumping systems with optimal control," *Journal of Dynamic Systems, Measurement, and Control*, vol. 140, no. 5, article 051004, 2017.

[27] F. J. Bu, "Analysis and solution of the wear mechanism of the pump," *Journal of Shengli Oilfield Staff University*, vol. 1, pp. 70–72, 2007, in Chinese.

[28] T. Dyck and A. Bund, "An adaption of the Archard equation for electrical contacts with thin coatings," *Tribology International*, vol. 102, pp. 1–9, 2016.

[29] S. M. Dong and B. S. Li, *Design of Sucker Rod Pumping System in Horizontal Wells*, Petroleum Industry Press, Beijing, China, 1996, in Chinese.